Current-assisted cooling in atomic wires

2009 J. Phys.: Condens. Matter 21 195304

(http://iopscience.iop.org/0953-8984/21/19/195304)

IOP Publishing Journal of Physics: Condensed Matter

J. Phys.: Condens. Matter **21** (2009) 195304 (5pp) doi:10.1088/0953-8984/21/19/195304

Current-assisted cooling in atomic wires

Eunan J McEniry, Tchavdar N Todorov and Daniel Dundas

Atomistic Simulation Centre, School of Mathematics and Physics, Queen's University Belfast, Belfast BT7 1NN, UK

E-mail: e.mceniry@qub.ac.uk

Received 8 December 2008, in final form 6 March 2009
Published 16 April 2009
Online at stacks.iop.org/JPhysCM/21/195304

Abstract

The effects of inelastic interactions between current-carrying electrons and vibrational modes of a nanoscale junction are a major limiting factor on the stability of such devices. A method for dynamical simulation of inelastic electron–ion interactions in nanoscale conductors is applied to a model system consisting of an adatom bonded to an atomic wire. It is found that the vibrational energy of such a system may decrease under bias, and furthermore that, as the bias is increased, the rate of cooling, within certain limits, will increase. This phenomenon can be understood qualitatively through low-order perturbation theory, and is due to the presence of an anti-resonance in the transmission function of the system at the Fermi level. Such current-assisted cooling may act as a stabilization mechanism, and may form the basis for a nanoscale cooling 'fan'.

(Some figures in this article are in colour only in the electronic version)

1. Introduction

The effects of inelastic interactions between the electrons and the nuclear degrees of freedom in current-carrying nanoscale systems have been extensively studied in recent years [1]. Such phenomena [2–5] have a strong influence on the conductance properties of nanoscale junctions and effects such as Joule heating and electromigration place limitations on the stability of such devices under current flow. In particular, the vibrational modes of nanojunctions can be often weakly coupled to those of the bulk, leading to a highly elevated effective vibrational temperature under current.

Here, we consider a model system that consists of an adatom bonded to an atomic wire. We illustrate numerically that the vibrational energy of the adatom may decrease under current flow and furthermore, within certain limits, that the rate of this cooling increases with increasing bias. We further show that this phenomenon may be understood qualitatively within low-order perturbation theory, and that the basis of the phenomenon is an anti-resonance in the transmission function of the junction at the Fermi level. Although the system envisaged here is a model one, the mechanism is generic and we hence propose that a system which possesses such a feature may form the basis for a nanoscale cooling 'fan'.

To perform the numerical simulations we use the correlated electron–ion dynamics (CEID) method. The method may be viewed as an extension of Born–Oppenheimer molecular dynamics to include approximately both correlations between electrons and ions and the quantum nature of nuclei. This amounts practically to an expansion of the exact equation of motion for the full density matrix of the combined electron–ion system about the mean classical trajectories of the ions [6, 7]. The expansion involves an infinite hierarchy of equations of motion for operators which correlate electrons to fluctuations in the ionic positions and momenta. In the approximation employed here, the equations are truncated to lowest non-trivial order in the electron–ion correlations and in the fluctuations of the ionic trajectories about the classical mean. The method has been used to examine inelastic current–voltage spectra in model systems [7] and, in combination with electronic open boundaries, to study the real-time heating and eventual equilibration of a dynamical ion with the current-carrying electrons [8].

2. The system

The system that we consider is shown in figure 1. It consists of a one-dimensional perfect atomic chain with a light adatom bonded to a single atom in the centre of the chain. The adatom is constrained to move in the direction perpendicular to the chain and is the only atom allowed to move. The system is described by a single-orbital nearest-neighbour orthogonal tight-binding model with parameters for gold [9], except the band filling which here is set to 1/2. The interatomic distance

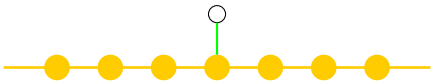

Figure 1. The adatom system discussed in the text.

within the chain is 2.5 Å, close to the equilibrium bond length for a perfect gold chain within the chosen tight-binding model. Following relaxation of the adatom-chain bond at zero bias, the adatom is positioned ∼2.41 Å above the chain. For these parameters, the hopping integral in the perfect chain is $H = -3.88$ eV and that between the adatom and the chain is $A = -4.49$ eV. Non-interacting electrons are assumed throughout. All onsite energies are set equal to zero.

We can obtain an insight into the conductance properties of the system by examining its elastic transmission function as a function of energy, shown in figure 2. The notable feature is the anti-resonance at the Fermi level, at the centre of the band, the origin of which is the interference of electron waves between the adatom and the chain. To see this, we consider the matrix elements of the electronic density-of-states (DOS) operator, $\hat{D}(E) \equiv [\hat{G}^-(E) - \hat{G}^+(E)]/2\pi\mathrm{i}$, where $G^{\pm}(E)$ are the retarded and advanced Green's functions of the system, within the space of the adatom, a, and the chain atom, c, below it:

$$D_{\mathrm{aa}} = -\pi^{-1}\, 2HA^2 \sin\phi/[(2HE\sin\phi)^2 + A^4]$$

$$D_{\mathrm{ac}} = -\pi^{-1}\, 2HAE \sin\phi/[(2HE\sin\phi)^2 + A^4]$$

$$D_{\mathrm{cc}} = -\pi^{-1}\, 2HE^2 \sin\phi/[(2HE\sin\phi)^2 + A^4].$$

Here ϕ and the energy E are related by $E = 2H\cos\phi$. For energies near the centre of the band ($E = 0, \phi = \pi/2$):

$$D_{\mathrm{aa}} \approx -\pi^{-1}\, 2H \sin\phi/A^2$$

$$D_{\mathrm{ac}} \approx -\pi^{-1}\, 4H^2 \cos\phi \sin\phi/A^3$$

$$D_{\mathrm{cc}} \approx -\pi^{-1}\, 8H^3(\cos\phi)^2 \sin\phi/A^4.$$

These may be compared with the DOS matrix elements within the end atom, call it 1, and the atom next to it, call it 2, for a semi-infinite perfect chain, with a hopping integral A:

$$d_{11} = -\pi^{-1} \sin\phi/A$$

$$d_{12} = -\pi^{-1}\, 2\cos\phi \sin\phi/A,$$

$$d_{22} = -\pi^{-1}\, 4(\cos\phi)^2 \sin\phi/A.$$

Thus, in terms of the energy dependence, the local electronic structure within the a−c complex in the adatom system mimics that within the two end atoms in a semi-infinite chain, which, in turn, is determined by the interference between incident and reflected waves. Another way to think of the anti-resonance is as a special case of a Fano resonance [10]: an effect arising from the coupling of a discrete level to a continuum,

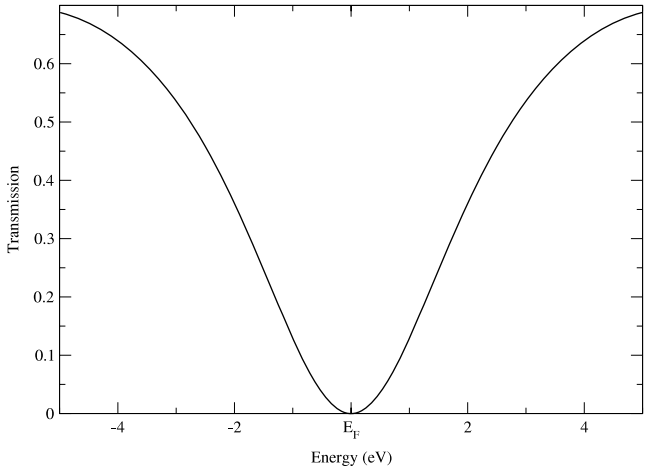

Figure 2. Transmission function for the adatom system. The feature of interest is the anti-resonance centred at the Fermi level $E_{\mathrm{F}} = 0$. The bias (the electrochemical potential difference) V in the simulations is symmetrically applied relative to the Fermi level.

whose occurence in mesoscopic systems has attracted recent attention [11–13].

The key feature is that D_{ac} and D_{cc}, like d_{12} and d_{22}, simultaneously vanish at the centre of the band. Moreover, at the centre of the band, the Green's function matrix element G^+_{cc} for the adatom system vanishes (as does g^+_{22} for the semi-infinite chain), which is the origin of the node in the transmission function,

$$T(E) = \frac{4(E/H)^2[1-(E/2H)^2]}{4(E/H)^2[1-(E/2H)^2] + (A/H)^4} \qquad (1)$$

at $E = 0$.

The low conductance at low biases suggests that the presence of electron–phonon interactions will provide an additional channel for conductance. To illustrate the effect of the electron–phonon interaction on the current, we run a series of CEID simulations at various voltages for a variety of initial oscillator temperatures, which correspond to different degrees of vibrational excitation of the adatom. The simulations use the electronic open-boundary method described in [8]. We take a 301-atom chain, with 100 atoms in each electrode, with the central 101 atoms of the chain forming the device region. The adatom is bonded to the central atom of the chain. With the mass of the adatom set to 1 amu, the Born–Oppenheimer zero-point energy of the adatom is $\frac{1}{2}\hbar\Omega_0 \sim 0.17$ eV. The open-boundary parameters of [8] are set to $\Gamma = 0.5$ eV, $\Delta = 0.01$ eV.[1] First, we consider the externally damped limit [14], in which the effective phonon occupation and the mean oscillator position are kept frozen in time. Figure 3 shows the elastic current–voltage spectrum, along with the current–voltage spectra obtained via the CEID formalism. It can be clearly seen that for this low-transmission system the effect of the electron–phonon interaction is to increase the conductance; furthermore, as the temperature of the oscillator increases, the effect on the current increases.

[1] The finite value of Δ leads to a slight thermal broadening of the electronic distributions which enter the device region.

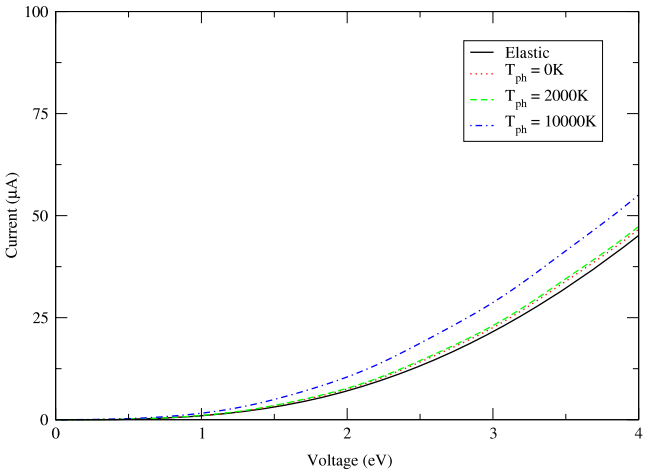

Figure 3. Elastic current–voltage spectrum for the adatom system along with inelastic current–voltage spectra obtained via the CEID method for a variety of initial oscillator temperatures, in the externally damped limit. $T_{\rm ph} = 2000$ K corresponds to a phonon occupancy of ∼0.2, $T_{\rm ph} = 10\,000$ K corresponds to an occupancy ∼2.

3. Vibrational energy under current

We next examine the response of the oscillator by unfreezing the ionic variables, and allowing the vibrational energy of the adatom to respond to the current-carrying electronic system. Again we consider a variety of initial effective ionic temperatures. Figures 4 illustrate the effect of the current on the vibrational energy[2], and the response of the current to the change in vibrational excitation.

In figure 4(a) with the oscillator initially in its ground state, we see that the effect of the current is to inject energy into the vibrational degree of freedom, in line with conventional current-induced heating. Since the oscillator is not connected to any other vibrational modes, its energy increases until it equilibrates with the electron gas. The current at a given bias is greater than in the earlier 'frozen-phonon' calculation, due to a small bias-induced relaxation of the adatom which slightly narrows the anti-resonance in the transmission function.

In figures 4(b), (c), where the oscillator is initially in an excited state, we notice that there is a decrease in the oscillator energy at low bias. Furthermore, as the bias is increased, the initial rate of cooling increases, indicating that an increase in current facilitates the cooling of the oscillator. As the bias is further increased, a crossover at which the rate of cooling has a maximum can be clearly seen. This phenomenon of current-assisted cooling acts as a stabilizing mechanism for the system, by helping to reduce the vibrational energy of the adatom. Curiously, due to the geometry of the system, no actual current flows through the bond connected to the adatom; there is just a bias-induced excitation of the local electronic structure.

[2] For the purposes of the present calculation, the vibrational energy of the adatom is defined as $U = C_{PP}/2M + K_{\rm BO}C_{RR}/2 + \bar{P}^2/2M$ where $C_{PP} = \langle(\hat{P} - \bar{P})^2\rangle$, $C_{RR} = \langle(\hat{R} - \bar{R})^2\rangle$, $\bar{R} = \langle\hat{R}\rangle$, $\bar{P} = \langle\hat{P}\rangle$ and $K_{\rm BO}$ is the Born–Oppenheimer spring constant. $\hat{R}$, $\hat{P}$ are the oscillator position and momentum operators. The contribution of the classical kinetic energy $\bar{P}^2/2M$ is much less than $C_{PP}/2M$. U here includes the zero-point vibrational energy.

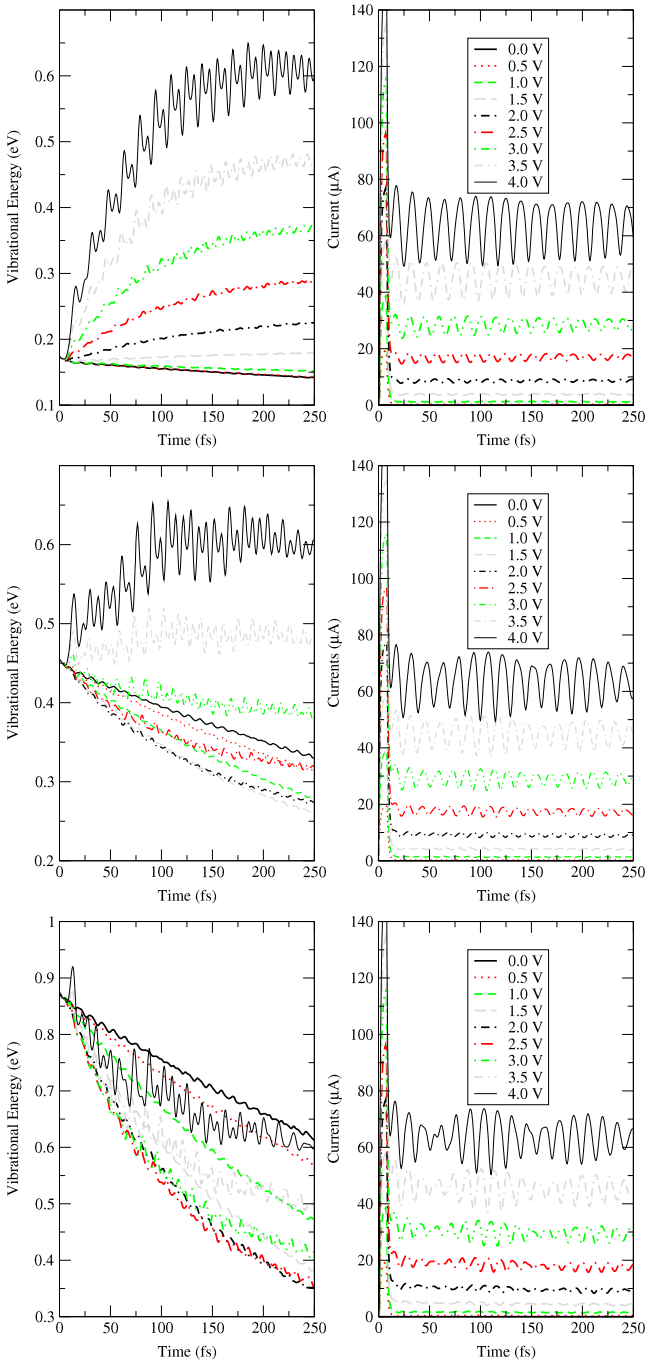

Figure 4. Vibrational energy (left) of the adatom at various biases as a function of time with corresponding current traces (right), for various initial oscillator temperatures. The initial step-like features in the current result from the transients following the application of the open boundaries [14]. From top to bottom, the initial oscillator temperatures are (a) $T_{\rm ph} = 0$ K, (b) $T_{\rm ph} = 5000$ K and (c) $T_{\rm ph} = 10\,000$ K.

A further point to note is that the equilibrium energy of the oscillator for a given bias is largely independent of the initial conditions of the oscillator; this energy is found by fitting the functional form $U(t) = U(t = 0) + U_1(1 - \exp(-t/\tau))$, where U_1 and τ are fitting parameters, to the data from the CEID calculations, from which the equilibrium energy is given by $U_{\rm eql} \approx U(t = 0) + U_1$. The equilibrium energy,

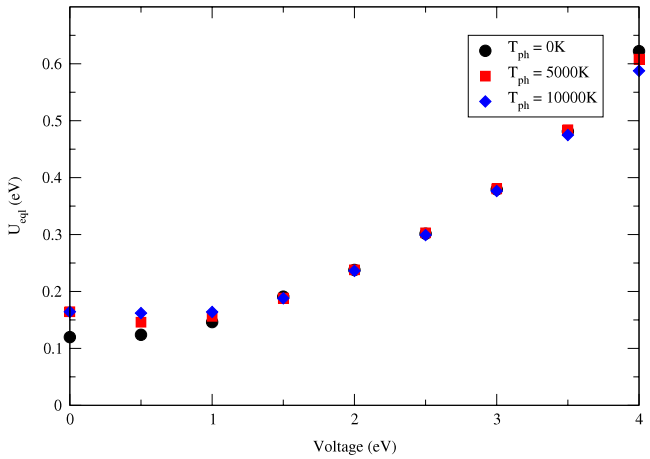

Figure 5. The oscillator energy, $U_{\rm eql}$, for equilibrium with the current-carrying electrons as a function of bias for the three initial oscillator temperatures considered. The plot illustrates that the equilibrium energy is essentially independent of the initial conditions.

shown in figure 5, increases as a function of bias but remains substantially lower than that for an ion in a ballistic chain for which $U_{\rm eql}(V) \sim eV/2$ [8].

4. Fermi Golden Rule

The above results can be explained qualitatively with the aid of the Fermi Golden Rule (FGR). Within the FGR, the rate of energy transfer $\dot{U}$ into a single vibrational mode of angular frequency Ω_0 can be written in the form [14]

$$\dot{U}(t) = -\kappa\left(U(t) - \frac{\hbar\Omega_0}{2}\right) + w_0 \qquad (2)$$

where $U = (N_{\rm ph} + \frac{1}{2})\hbar\Omega_0$, with $N_{\rm ph}$ related to the effective phonon temperature via $N_{\rm ph} = [\exp(\hbar\Omega_0/k_{\rm B}T_{\rm ph}) - 1]^{-1}$. It can be shown [14] that the quantity κ (which characterizes the energy loss from the vibrations to the electrons) largely depends on the local electronic structure at the edges of the available energy window for conduction, while w_0 (which controls the heating of the vibrations) collects contributions from the full conduction energy window. As a consequence of the suppression of the DOS operator matrix elements $D_{\rm ac}$ and $D_{\rm cc}$ at $E_{\rm F}$, the coupling of the adatom to conduction electrons at those energies is weak. Conversely, at energies away from $E_{\rm F}$, this coupling is enhanced. As a result, at low bias, κ is suppressed; as the bias is increased, the Fermi levels of the left and right electrodes move into regions of improved electronic coupling, and κ hence increases. The oscillator energy for equilibrium with the current-carrying electrons (in the absence of lattice heat conduction), $U_{\rm eql}(V) = w_0(V)/\kappa(V) + \hbar\Omega_0/2$, increases with bias (as shown in figure 5), but remains substantially lower than that for an ion in a ballistic chain. Rewriting equation (2) as

$$\dot{U}(t) = -\kappa(V)(U(t) - U_{\rm eql}(V)), \qquad (3)$$

we see that, for $U(t = 0)$ sufficiently larger than $U_{\rm eql}(V)$, the initial cooling rate, $\dot{U}(t = 0)$, should increase with moderate increases in bias, and the relaxation of U down towards $U_{\rm eql}(V)$ speeds up. This is the origin of the current-assisted cooling seen in the dynamical simulations.

We note that the present system is the converse of that considered in [14], namely a system with a narrow *resonance* at the Fermi level. In that case, $\kappa(V)$ decreases with bias, while $w_0(V)$ saturates. In the limit of perfectly trapped phonons, this leads to a substantial enhancement of both the maximal heating and the phonon–electron equilibration time for voltages which engulf the resonance, compared with a resonance-free system.

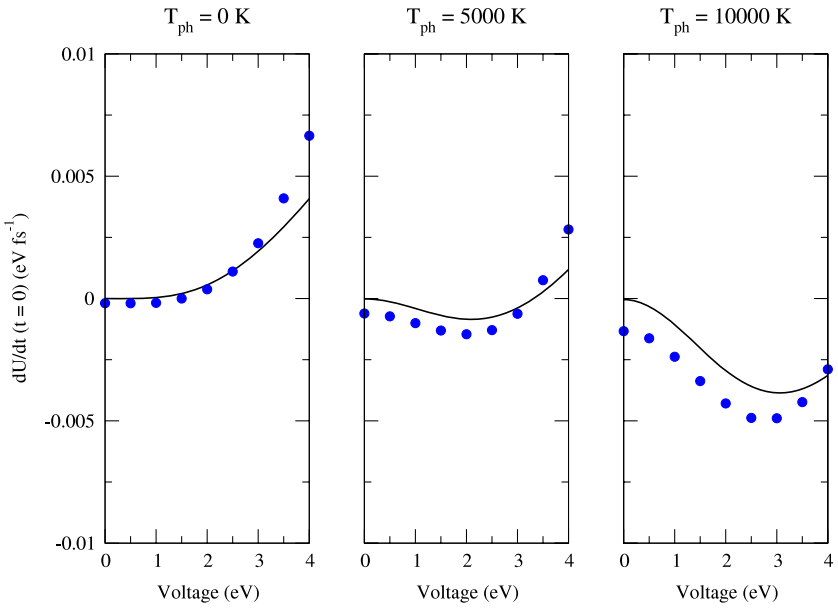

Figure 6. $\dot{U}(t = 0)$ for the adatom system within the Fermi Golden Rule (solid line), for a variety of effective initial oscillator temperatures. The dots are obtained from a fit to the CEID calculations.

To explore this further, we use the FGR to calculate the heating rates for the adatom system, within the same tight-binding model as in the CEID calculation, with an electronic structure computed within the Landauer formalism for an infinite perfect chain, with the adatom in the relaxed position at zero bias[3]. The result for $\dot{U}(t = 0)$ is compared with that from the CEID calculation which, using the fitting procedure above, is given by $\dot{U}(t = 0) \approx U_1/\tau$. The reasonable agreement in the qualitative trends is illustrated in figure 6. Possible reasons for the differences between the two calculations are the small bias-induced relaxation in the average adatom-chain bond length and the higher-order electron–phonon coupling implicitly present in the dynamical simulation, as well as the loss of energy resolution due to the approximate open-boundary method in the CEID calculation [8].

We have demonstrated the basis for a nanoscale device in which the bias assists the energy relaxation of a hot ion, by enhancing its coupling to the conduction electrons. A detectable signature of the underlying electronic structure that enables the effect is the anti-resonance in the transmission function. The resultant model device constitutes a notional current-controlled cooling fan for the hot ion.

Although we have considered only a simple model system, we expect the key findings to be reasonably robust with the details of the calculation, at least within the present model setup. We do not expect the effect to change qualitatively with variations in the band filling in the chain, provided that the energy level on the adatom remains pinned against E_F. Variations in the adatom-chain hopping integral would alter the width of the anti-resonance, and hence the voltage scale for the current-assisted cooling in figure 6. Finally, if the mass of the adatom is sufficiently small, that would help to decouple its motion from that of the other atoms in the system, bringing us closer to the model scenario assumed here.

[3] The FGR calculation uses equation (C1) in [14]. The derivative of the adatom-chain hopping integral with distance is $4 \times 4.49/2.41$ eV Å^{-1}. The electronic temperature in the Fermi–Dirac functions was set to zero.

Acknowledgments

This work was funded by the Engineering and Physical Sciences Research Council (UK) under grant No. EP/C006739/01. This work made use of the facilities of HPCx, the UK's national high-performance computing service, provided by EPCC at the University of Edinburgh and by CCLRC Daresbury Laboratory, and funded by the Office of Science and Technology through EPSRC's High End Computing Program.

References

[1] Galperin M, Ratner M A and Nitzan A 2007 *J. Phys.: Condens. Matter* **19** 103201
[2] Agraït N, Untiedt C, Rubio-Bollinger G and Vieira S 2002 *Phys. Rev. Lett.* **88** 216803
[3] van den Brom H E, Yanson A I and van Ruitenbeek J M 1998 *Physica* B **252** 69
[4] Smit R H M, Untiedt C and van Ruitenbeek J M 2004 *Nanotechnology* **15** S472
[5] Tsutsui M, Kurokawa S and Sakai A 2006 *Nanotechnology* **17** 777
[6] Horsfield A P, Bowler D R, Fisher A J, Todorov T N and Sánchez C G 2004 *J. Phys.: Condens. Matter* **16** 8251
[7] Horsfield A P, Bowler D R, Fisher A J, Todorov T N and Sánchez C G 2005 *J. Phys.: Condens. Matter* **17** 4793
[8] McEniry E J, Bowler D R, Dundas D, Horsfield A P, Sánchez C G and Todorov T N 2007 *J. Phys.: Condens. Matter* **19** 196201
[9] Sutton A P, Todorov T N, Cawkwell M J and Hoekstra J 2001 *Phil. Mag.* B **81** 1833
[10] Fano U 1961 *Phys. Rev.* **124** 1866
[11] Li J, Schneider W-D, Berndt R and Delley B 1998 *Phys. Rev. Lett.* **80** 2893
[12] Kobaysahi K, Aikawa H, Katsumoto S and Iye Y 2002 *Phys. Rev. Lett.* **88** 256806
[13] Katsumoto S 2007 *J. Phys.: Condens. Matter* **19** 233201
[14] McEniry E J, Frederiksen T, Todorov T N, Dundas D and Horsfield A P 2008 *Phys. Rev.* B **78** 035446